Plasticity of the gastrocnemius elastic system in response to decreased work and power demand during growth

Cox, SM[1,2], DeBoef, A[2,3], Salzano, MQ[2,4,5], Katugam, K[2], Piazza, SJ[2], Rubenson, J[2,4]

[1]The Department of Ecology and Evolutionary Biology, The University of California, Irvine, CA, [2]Biomechanics Laboratory, Department of Kinesiology, The Pennsylvania State University, University Park, PA, [3]The Department of Biological Sciences, Georgia Institute of Technology, Atlanta, GA, [4]Integrative and Biomedical Physiology, The Pennsylvania State University, University Park, PA, United States [5]Department of Kinesiology, The University of Massachusetts - Amherst, Amherst, MA

Abstract

Elastic energy storage and release can enhance performance that would otherwise be limited by the force-velocity constraints of muscle. While functional influence of a biological spring depends on tuning between components of an elastic system (the muscle, spring, driven mass, and lever system), we do not know whether elastic systems systematically adapt to functional demand. To test whether altering work and power generation during maturation alters the morphology of an elastic system, we prevented growing guinea fowl (*Numida Meleagris*) from jumping. At maturity, we compared the jump performance of our treatment group to that of controls and measured the morphology of the gastrocnemius elastic system. We found that restricted birds jumped with lower jump power and work, yet there were no significant between-group differences in the components of the elastic system. Further, subject-specific models revealed no difference in energy storage capacity between groups, though energy storage was most sensitive to variations in muscle properties (most significantly operating length and least dependent on tendon stiffness). We conclude that the

gastrocnemius elastic system in the guinea fowl displays little to no plastic response to decreased demand during growth and hypothesize that neural plasticity may explain performance variation.

Introduction

Taking advantage of storage and release of elastic strain energy can enhance performance that would otherwise be limited by the force-velocity constraints of muscle. The temporal decoupling of energy production from energy delivery permitted by elastic energy storage allows muscles and tendons to produce force effectively over a range of shortening or lengthening speeds. Muscles may generate forces during slow or isometric contractions and elastic recoil augments the rate of energy delivery or absorption during rapid movements [1,2]. By making use of energy storage in the tendon "spring", a muscle tendon unit (MTU) can produce force more economically or with greater power than a muscle alone [2]. Yet, several studies have identified important differences among spring-muscle combinations. Wilson, Lichwark, and colleagues [3,4] showed that the efficiency of an MTU during cyclic loading depends on the tuning of relative muscle and spring properties. For instance, muscle efficiency varies with both fascicle length and tendon stiffness, with the specific optimal efficiency values depending on gait conditions [3]. Several researchers [5–9] have shown that the opposing inertial or drag forces acting on a motor-spring system also influence whether springs enhance performance. Adding further complexity, Sawicki and colleagues [10,11] found that the timing of neural activation of muscle during hopping must be tightly controlled to take advantage of in-series springs. Together, this body of work suggests that understanding the conditions in which spring systems enhance performance may require expanding our focus from the muscle-tendon unit to that of the broader 'elastic system' which includes the muscle (motor), the spring, the resistive forces, and the neural control of the system. The optimal performance of an elastic system may

require tuning of both morphology and neural control. This approach recognizes the integrated nature of the neuro-musculoskeletal system[12].

The sensitivity of elastic system efficiency to the tuning of its components complicates inferences for how elastic systems systematically adapt to functional demand during maturation. For instance, do growing individuals who regularly perform functions that utilize elastic strain energy develop elastic systems with greater energy storage capacity? This is still unknown because most studies of MTU plasticity have focused on how individual components of elastic systems (neural control [13–15], muscle [16–19] and tendon [20–25]) vary with task or training, and how those individual changes influence function of a muscle-tendon unit [10,11,26–28]. Yet, the integrated nature of the elastic system suggests that functional consequences of plasticity are difficult to predict by analyzing elements in isolation [27,29,30]. Therefore, the complex nature of the neuromuscular adaptation of elastic systems may require analysis at the system level rather than at the level of individual components.

Here we present a study of the morphological plasticity of an elastic system. Specifically, we ask whether individuals that jump during maturation (an activity requiring elastic energy storage and return [31]) develop elastic systems that more capable of storing elastic strain energy at maturity than those of individuals restricted from jumping. Here we focus on the elastic system most involved in storage and release of elastic energy during jumping[32–36], the gastrocnemius elastic system. We test this by altering the rearing conditions of two groups of guinea fowl (*Numida meleagris*) across the entire growth period, allowing one group to engage in jump-to-perch behavior and preventing all jumping in the other group. We previously reported that restricted birds in this study showed detriments in jump performance at adulthood [37]. In this manuscript, we aim to link the morphological and functional consequences of our intervention.

Of the morphology data, we take both an individual-component and systems-level approach to evaluate the plasticity of an elastic system during growth. At the component level, we probe whether our treatment resulted in systematic morphological differences in individual components of the gastrocnemius elastic system between groups. We seek to determine whether components of this elastic system plastically adapt to variations in functional demand during growth. At the systems level, we ask how plastic changes at the component level interact to influence the capacity for elastic energy storage. To do this, we developed subject-specific musculoskeletal models that incorporated experimentally measured morphological properties of each bird's elastic system. With each subject-specific model, we simulated a fully activated muscle contraction under various postures and quantified the resulting tendon energy stored. The purpose of this systems-level analysis was to evaluate the integrated effects of morphological variation.

The component-and systems-level analyses serve as a case study for understanding how a particular elastic system changes with functional demand. We also took advantage of the variation within and across groups to ask broader questions about the relationship between form and function in elastic systems. Specifically, we asked which combinations of naturally occurring morphological variation most influence the ability of an elastic system to store energy. Lastly, we probed the extent to which energy storage capacity in the gastrocnemius elastic system correlated with jump performance.

We hypothesize that components of an elastic system plastically adapt to variations in functional demand during maturation, resulting in greater energy storage capacity in birds that jump during growth. We predict energy storage capacity will increase linearly with muscle force-generating capacity and inversely with tendon stiffness [38–40]. Finally, we predict that differences in jump performance positively correlate with an animal's ability to store elastic strain energy in the tendon of the gastrocnemius elastic system.

Methods

Experimental Protocol

Animals. To study these questions, one-day-old guinea fowl keets (*Numida meleagris*) were obtained from a regional breeder (Guinea Farm; New Vienna, IA). After a 2-wk brooding period, the keets were pen reared through skeletal maturity (>6 months) in one of two conditions, as we previously described in detail (Cox et al 2020). A control group (C; n =8) was housed in a large, circular pen (3.14 m^2) that allowed ample room for locomotion and objects for jumping and perching. The restricted treatment group (R; n = 7) were raised a smaller pen (1 m^2 at maturity) with low mesh ceilings that prevented jumping. Food and water were available *ad libitum* (food intake did not differ between groups). Lights were programmed to be on a 12:12-h light-dark cycle. The experimental protocol was approved by Institutional Animal Care and Use Committee at The Pennsylvania State University (IACUC; Ref. #46435).

Movement Analysis. As described previously [37], to quantify the influence of pen configuration on the movement patterns of both treatment groups, pens were filmed from above for ten minutes, four times per day, across the growth period (Foscam; C2 1080p HD cameras, Houston, TX). For each bird in the pen, behaviors were tracked and categorized into two states (standing or walking) and three events [short sprint (<2 sec), hurdle jump (< body height) and perch jump (~2 x body height).

Functional Measures

As described previously [37], jump performance was measured by placing each bird in turn on 6x6 in. force plates (AMTI HE6x6; Watertown, MA, USA) enclosed in a tapered box and encouraging the birds to jump. Jump power was calculated from the instantaneous net vertical ground reaction and the vertical center of mass velocity. Velocity was obtained by integrating the center of mass

acceleration, which was in turn found from the net ground reaction force and the body mass. We calculated jump work by integrating the instantaneous power with respect to time over the course of the jump.

Quantification of properties of individual components of the elastic system

Specimen muscle architecture preparation. The pelvic limb was separated from the upper body and the left and right legs were then split by sectioning the pelvis at the midline while avoiding muscle attachments. Right limbs were placed into neutral buffered formalin for fixation (10%) for at least two weeks, while left legs were fresh-frozen and kept at -20 °C. Right limbs were positioned with joint angles approximating those at mid-swing during running (hip: 30°, knee: 80°, ankle: 125°, within ±2° [41]). Joint angles were confirmed for the fixed limbs using photographs made with a digital camera (Canon EOS550D; Surrey, United Kingdom) and analyzed with ImageJ (National Institutes of Health, Betesda, MD). Left limbs were fresh-frozen and saved for later muscle mass measures.

Muscle Analyses. We made measurements of the lateral and medial heads of the gastrocnemius muscle (LG and MG), the muscle group of the MTU thought primarily responsible for storage and release of elastic strain energy during running and jumping [31,36]. The third (intermedia) head of the gastrocnemius only comprises ~10% of the total mass of the gastrocnemius muscles in this species [42] and thus was not included in the analysis. MG and LG were dissected from the fresh-frozen left limbs and weighed to the nearest 0.1 milligram. The LG and MG were then dissected from the fixed limbs for fascicle length, pennation angle, and sarcomere analysis. LG was first split longitudinally through the mid-belly to view fascicle arrangement. Photographs of whole MG and split LG made with a digital camera (Canon EOS550D) were imported into ImageJ for

measurement of the pennation angle between muscle fascicles and their insertions on the aponeurosis [43].

Due to the expected within-muscle heterogeneity of strain [44,45], each muscle was divided into sections for analysis. MG was split into anterior and posterior fascicles [46] and then again split proximally/distally, resulting in four sections. The LG was split into proximal, middle, and distal sections, each spanning one-third the length of the muscle belly. Average pennation angle was found for each section by taking the mean of three angle measurements. Sarcomere lengths for each section were found using the laser diffraction techniques described in [43]. A minimum of three sarcomere length measurements were taken from each muscle fascicle bundle and these measurements were averaged to obtain the mean measured sarcomere length.

Optimal fascicle length, L_O, was calculated by multiplying the length of the fascicle by the ratio of optimal sarcomere length of guinea fowl muscle (2.36 μm; [46]) to the mean measured sarcomere length.

Pennation angle at optimal fascicle length, θ_{OFL}, was calculated from the average measured pennation angle, $\bar{\theta}$, and the ratio of measure fiber length, F_l, and calculated optimal fascicle length, L_O according to the equation [47]:

$$\theta_{OFL} = \sin^{-1}\left\{\frac{F_l \sin\bar{\theta}}{L_O}\right\} \quad (1)$$

Maximum isometric force along the muscle fiber for the MG and LG were calculated from the muscle mass, m, optimal fascicle length, L_O and muscle density (ρ_{musc} = 1060 kg/m^3 [48] using the specific tension, f (3 x 10^5 N/m^2, Rospars and Meyer-Vernet, 2016), according to the equation:

$$F_{max} = \frac{f * m}{\rho_{musc} L_0} \quad (2)$$

We specifically calculated isometric force along the muscle fiber for input into the musculoskeletal model rather than including the influence of pennation angle because pennation angle is a separate input into the OpenSim Millard muscle model (see below for model description), which accounts for the change in pennation angle with muscle length [50]. For statistical tests, muscle force along the tendon was analyzed.

Moment Arm. Gastrocnemius moment arm at the ankle was experimentally measured using the tendon travel method [51,52] as described by Salzano (2020). The gastrocnemius moment arm at the ankle was experimentally measured using the tendon travel method as described by Salzano [53]. In short, the Achilles tendon was attached to a linear transducer (Model P510-2-S11-N0S-10C, UniMeasure, Inc., Corvallis, OR) to measure excursion and kept at a constant 10N tension to prevent changes in tendon strain (Figure 1). Retroreflective markers were placed on dissected limbs to track the relative movement of the tibia and tarsometatarsus in 3D across a range of joint angles using a 4-camera Motion Analysis system

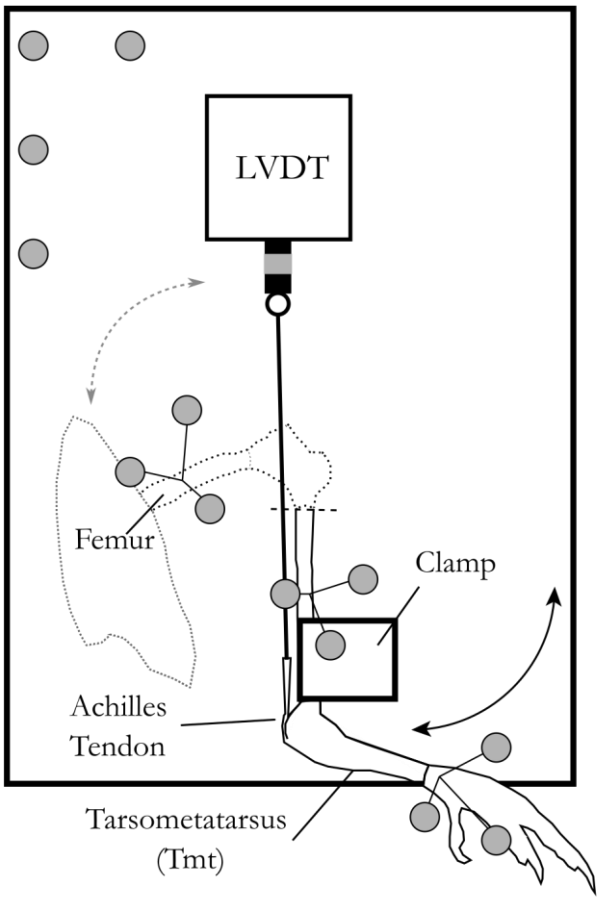

Figure 1: Setup for the tendon travel experiment. The limb was positioned so that the tibiotarsus was held firm by a 3D printed clamp. In the knee joint motion trial, the femur was rotated to move the knee through its ROM. The tibiotarsus was then cut to remove the proximal portion of the limb, allowing for LVDT to be attached to the Achilles tendon. For tendon travel trials, the TMT was rotated to move the ankle through its ROM. Gray coloring represents retroreflective markers on the limb and LVDT. The dotted line outlines the pelvis femur, and knee, which were removed after the knee joint motion trial. The dashed line represents location at which the tibiotarsus was cut after the knee joint motion trial. Figure adapted from Salzano, 2020.

(300 Hz; Kestrel, Motion Analysis Corporation, Santa Rosa, CA), and automatically synchronized to the linear transducer data within the motion analysis software (Cortex , Motion Analysis Corporation). Joint centres and a mean helical axis were calculated from motion data for each trial and used to calculate flexion angle at the ankle at each timepoint [54]. A cubic spline was fit to the tendon excursion versus flexion angle points using least-squares approximation and tendon excursion was differentiated with respect to angle to estimate moment arm across the measured range of motion (30°-90°). Average values are reported in Table 1.

Tendon force-length curves. We quantified the tendon force-length properties with material analysis as described in [25]. In short, tendons were detached from the gastrocnemius muscles but left attached at their insertion points on the tarsometatarsus bone. Both the bone and the tendon's proximal end were connected to a material testing machine (858 Mini Bionix II; MTS Systems Corp; Eden Prairie, MN, United States). Samples were mounted vertically using custom clamps on the tendon aponeurosis and the TMT and attached to a 50-pound load cell (MTS Systems Corp; Eden Prairie, MN, United States). The upper clamp gripped the entire aponeurosis of each sample, leaving only the free tendon exposed to loading. The tendon force-length properties were quantified by loading the tendon cyclically (20 cycles) to 4% strain. The tendon force-length curves were calculated by averaging the data from last 5 cycles of the loading protocol. Tendon force-strain curves were calculated by normalizing displacement by the length of the tendon, T_L, measured to the nearest 0.1 mm with calipers while under zero force in the material testing setup. Average values for tendon stiffness given in Table 1 were calculated from the slope of the tendon force-length curve across the last 50 points measured in the last 5 cycles of trials, at strain between 3 and 5%.

Tendon Slack Length. The tendon slack lengths for the LG and MG were estimated from experimental measures as described in Appendix A. Because model based estimates of muscle fiber length in a

198 given posture are particularly sensitive to the tendon slack length [55–57] and our calculations
199 involved several simplifying assumptions, we further refined our experimental estimates of tendon
200 slack length by fine-adjusting the tendon slack length parameter in the OpenSim model (see
201 Appendix A for experimental tendon slack length measurement and see below and Appendix B for
202 model development). After experimental moment arms and tendon and muscle properties were
203 added to subject specific models, each model was posed in the individual's fixed posture. The
204 model's tendon slack length was adjusted iteratively in the model until the LG and MG normalized
205 fiber lengths were within 1% of the experimentally measured values. These final values are listed in
206 Table 2.

207 **Quantifying the influence of restricted jumping on energy storage capacity**

208 We generated a flock of subject-specific musculoskeletal models by modifying the generic model
209 [58] to match experimental values measured for each bird (see Appendix B). With these models, we
210 quantified the capacity of each subject-specific model to store elastic energy in its Achilles tendon
211 across a range of joint postures [Ankle^{o} : 31 to 145, Knee^{o}: -145 to -15, Figure 2 [58])]. At each
212 posture, the simulated LG and MG were activated at 100% and the muscle-tendon unit was
213 equilibrated with the OpenSim MATLAB equilibrateMuscles() function, which adjusts muscle and
214 tendon length such that tendon force and muscle (active and passive) forces balance. The LG and
215 MG insert on the same tendon but, due to OpenSim modeling constraints, these muscles are
216 modeled as having separate tendons. To calculate the stored elastic energy in the combined Achilles
217 tendon, then, we first extracted the resulting force, f_a, along the tendon for each muscle. These
218 values were summed and the resulting tendon strain in a single tendon, $\in_{Ta}$, was found from the
219 inverse of the experimentally measured force-strain curve.

$$\varepsilon_{Ta} = g^{-1}(f_a). \quad (3)$$

The strain energy stored in the strain of the tendon, *PE* (eq. 10), was calculated by integrating the tendon force-strain curve from zero to the calculated strain and multiplying that by the tendon sample length, L_T, as measured at zero strain during the material testing.

$$PE = L_T \int_0^{\varepsilon_{Ta}} g(\varepsilon)\, d\varepsilon \quad (4)$$

Simulations of 100% activation of the LG and MG were performed across the range of experimentally measured joint angles for the ankle and knee joint (Figures 2A&B). From these simulations, we extracted the maximum elastic energy storage across all postures for each bird and the ankle and knee angles at which the maximum was achieved, and recorded the values in a pre-jump posture (Figure 2C, [31]). Tendon elastic energy stored in the pre-jump posture has been found to be a requirement for the very high power generated in guinea fowl jumping [31,37]. Additionally, we recorded the normalized fiber length for each muscle at this posture at zero activation.

Statistical Tests

To determine whether components of the gastrocnemius elastic system change systematically in response to changes in demand, we evaluated the influence of treatment group (restricted vs. control) on each element of morphology measured. This was accomplished using t-tests if the homogeneity of variance assumption test was passed and using a Kruskal-Wallis test by ranks when this criterion was not met. Non-parametric analyses are indicated with an asterisk after the p-value in Tables 1&2. The threshold for statistical significance was set at 0.005 after a Bonferroni correction for multiple comparisons. Likewise, the relationship between treatment group and elastic

239 energy storage capacity was evaluated with a t-test after data passed tests for normality and
240 homogeneity of variance, as described above for evaluation of differences between groups of
241 individual elastic system components.

242 We used stepwise comparison of Akaike information criterion (AIC) values [stepAIC R Mass
243 package [59]] to determine the parameters and coefficients of the full model that best predicted
244 elastic energy storage potential across natural variation of joint postures in preparation for jumps.
245 The full statistical model evaluated included stored strain energy, *PE*, as a dependent factor and, as
246 potential independent variables, tendon stiffness, *tendonK*, the summed maximum isometric force
247 capacity of LG and MG along the tendon, *sumFMax*, the average LG and MG optimal fascicle
248 length, *AvOFL*, and starting muscle length at zero activation of the LG and MG in the pre-jump
249 posture, *AvLenA0c*. We included possible interaction terms between muscle force capacity, tendon
250 stiffness and muscle start length (*sumMaxF*tendonK*AvLenA0c*) and between optimal fascicle length
251 and tendon stiffness (*avOFL*tendonK*) following recommendations by Zajac [60] of functional
252 equivalent muscle tendon joint properties. We did not include muscle moment arm or tendon slack
253 length in the statistical model because they both contributed to the starting muscle length at any
254 given joint posture.

255 To quantify the relative explanatory power of morphological variation of any individual element to
256 predict stored energy to a systems level approach, we compared individual parameter models to the
257 best multi-parameter model found by stepwise comparisons described above. The AIC value of the
258 best model was compared to AIC values of models with individual predictors and their relative
259 explanatory power computed [61] .

260 The relationship between Achilles tendon elastic energy storage capacity and experimentally
261 measured muscle-mass-normalized peak power output and jump work were both tested with a linear

262 model with elastic energy storage as the dependent variable and peak power or jump work as the

263 independent variable. See [62] for details on how power and work were calculated from force plate

Table 1: Morphological and functional measures by treatment. All values are given as means +/-standard deviations. 'pVal' column lists the p-value of statistical comparisons between groups. Bolded rows show statistically significant differences between groups. * indicates data reproduced from Cox et al. (2020).

	Restricted	Control	pVal
Total animals	8	8	
Body mass kg	1.7±0.11	1.7±0.14	0.5
Extensor muscle mass kg	0.239(0.022)	0.257(0.02)	0.18
Average moment arm cm	0.91±0.05	0.94±0.03	0.24
Tendon stiffness kN/m	48.1±13	53.5±10	0.39
Leg length mm	345±11	349±18	0.56
Femur length/leg length	0.25±0.01	0.25±0.01	0.18
Tibia length/leg length	0.36±0.01	0.35±0.01	0.1
Tmt length/leg length	0.22±0.01	0.22±0.01	0.55
Toe length/leg length	0.17±0.01	0.17±0.01	0.63
*Jumps/day during growth	0	194(349)	
At maturity			
***Max jump takeoff velocity m/s**	**3.3±0.43**	**4.0±0.36**	**0.007**
***Jump work J/kg**	**37±9.2**	**50±8.4**	**0.013**
***Peak power W/kg**	**787±165**	**1171±117**	**3.5e-4**
***Peak jump force/body weight N/N**	**4.7±0.54**	**6.7±0.74**	**5e-5**

264 data.

265 # Results

266 ## Variation in individual elements of the elastic system

267 We found no statistically significant differences in any individual morphological property between

268 birds that jumped during growth and those that did not (all p>= 0.1, Tables 1&2).

269

270 ## Energy storage capacity between groups

271 We found no significant differences in the capacity to store energy in the strain of elastic elements

272 between birds restricted and unrestricted from high power activities during maturation, despite

small differences in tendon strain that did not reach significance (Table 3, Figure 3). This held true both at the peak crouched posture before jump initiation (Figure 2C, p=0.43) and at the posture that optimized elastic energy storage (Figure 2D, pVal=0.44). It should be noted that the optimum posture for elastic energy storage was at the most extended knee angle and the most flexed ankle angle tested and was ~85° more extended ankle angle than birds used in preparation for a jump. While this more extended posture lengthened the gastrocnemius and increased the energy stored in the Achilles, it shortened the operating length of the knee extensor muscles, reducing their force-generating capacity. In the prejump posture, the shorter gastrocnemius length decreases elastic storage capacity by 12% for control birds and 10% for restricted birds (Table 3) in comparison to the optimal posture for energy storage.

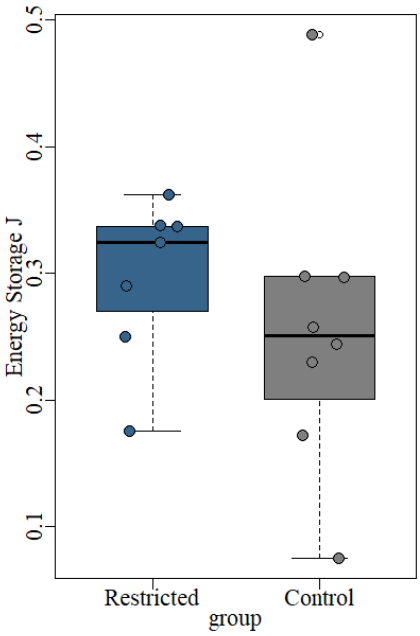

Figure 3: Restricting high power activities does not decrease or significantly influence the capacity to store elastic strain energy. Each dot represents data from one individual.

Morphological predictors of elastic energy storage capacity

Table 2: Muscle morphological data by treatment for the lateral (LG) and medial (MG) gastrocnemius muscles: Muscle mass (Mass g), optimal fascicle length, (L_O mm), Maximum Isometric Muscle force (Max Iso Force N), muscle pennation angle at optimal fiber length (Penn Ang rad), and tendon slack length (Tendon SL mm). Morphological measures did not vary between groups. All values are given as means +/-standard deviations. pVal column lists the p-value of statistical comparisons between groups.

		Restricted	Control	pVal
LG	Mass g	9.0±1.3	9.2±1.5	0.77
	L_O mm	24±2.9	24±4.1	0.95
	Max Iso Force N	105±15	110+-22	0.64
	Pen Ang rad	0.33±0.05	0.30±0.07	0.38
	Tendon SL mm	135±7.3	139±6.5	0.32
MG	Mass g	11±1.4	12±1.8	0.2
	OFL mm	28±4.2	29±3.5	0.81
	Max Iso Force N	108±20	118±29	0.44
	Pen Ang rad	0.20±0.03	0.21±0.03	0.51
	Tendon SL mm	150±8.3	150±9.1	0.97

Table 3: Comparison of energy storage capacity and normalized fiber length between restricted and unrestricted birds at maturity across all postures and in the pre-jump posture (shaded grey). Normalized muscle length at the start and end of contraction designated by Average n.Fiber length at A0 and A100 respectively.

		Restricted	Control	pVal
At max strain energy posture	Energy Storage Potential J	0.3±0.065	0.26±0.12	0.44
	Tendon Strain	0.12±0.016	0.098±0.021	0.031
	Average n.Fiber length at A0	1.1±0.051	0.99±0.098	0.11
	Average n.Fiber length at A100	0.75±0.051	0.72±0.054	0.27
	Knee Angle at Max PE°	-131±1.9	-130±0	1
	Ankle Angle at Max PE°	-45±0	-45±0	1
In pre-jump posture (Knee: -135 Ankle: 120)	Energy Storage Potential J	0.27±0.055	0.23±0.11	0.43
	Tendon Strain	0.12±0.015	0.094±0.021	0.028
	Average n.Fiber length at A0	1±0.05	0.96±0.097	0.11
	Average n.Fiber length at A100	0.73±0.048	0.7±0.051	0.28

289

290 We found that the amount of energy stored in strain of the tendon was best explained by variation

291 in the average of the passive LG and MG muscle length at activation onset, *avLenA0* (Table 4).

292 Figure 4A illustrates that tendon strain energy increases at longer starting lengths both between

293 individuals and, even more strikingly within individuals, across postures. Muscle force capacity along

Table 4: Results of models comparing how well variation of individual elastic elements explain variation in elastic storage potential (dark shaded grey regions) and stepwise model comparisons of models with multiple predictors (lighter shaded region) find that muscle operating length at the start of activation (AvLenA0) is most predictive of energy storage, with muscle force capacity, the sum of lateral and medial maximum isometric force (Force), and average gastrocnemius optimal fiber length, avOFL, also significant.. Tendon stiffness, Tendon K, add little to no additional predictive information. A multi-predictor model (Full:, darker shaded region), explained variation in energy storage capacity over 160,000 times better than any individual predictor. Likelihood comparisons between the null and individual models are designated by L(null|x), and between the full model and individual predictor models by L(full|x). Akaike weights are listed under w(AIC)

	Coeff	**Adj. R^2**	**pVal**	**AIC**	**ΔAIC (1-5)**	**w(AIC)**	***L*(null|x)**	**ΔAIC (2-6)**	**w(AIC)**	***L*(full|x)**
1. Null:				-28	0	1.1e-5	1			
2. Force	0.002	0.50	2.0e-3	-37	-9.4	1.2e-3	111	28	1.6e21	1.0e6
3.tendon K	-1.3e-8	-0.077	1	-26	2.0	3.1e-6	0.37	39	5.3e18	3.0e8
4.AvLenA0	0.40	0.57	6.4e-4	-40	-12	3.3e-3	390	25	5.6e21	2.8e5
5. avOFL	-1.5	0.26	3.1e-2	-31	-3.6	5.1e-5	6	33	8.6e19	1.9e7
6.Full:		0.93	2.3e-6	-65				0	1.5e27	1
FMax	6.1e-3		3.2e-4							
tendon K	1.2e-5		0.02							
AvLenA0	0.29		2.0e-4							
avOFL	0.78		0.07							
Force* tendonK	-7.1e-8		4.5e-3							

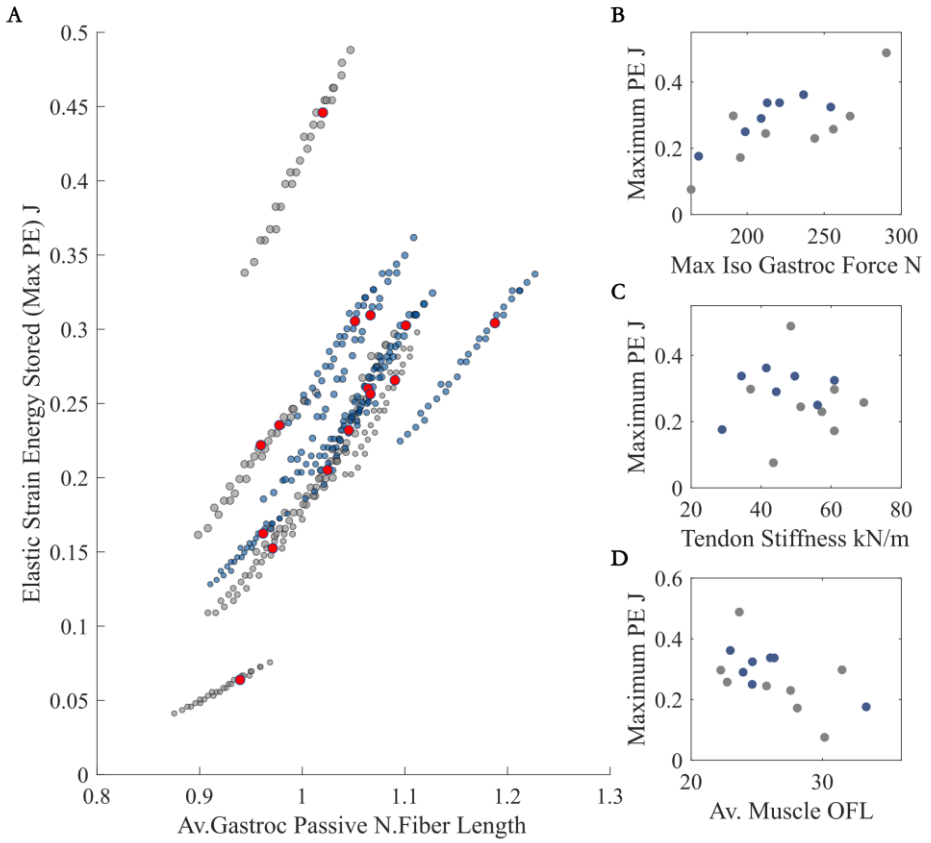

Figure 4: Energy stored in the tendon increases with passive normalized fiber length (length at onset of muscle activation) across different postures (A) and muscle force capacity (B), decreases with muscle optimal fiber length (D), but did not consistently vary with tendon stiffness (C). The variable that most predicts elastic strain energy is muscle normalized fiber length at activation onset (A), with muscles operating at longer lengths enabling greater elastic energy storage. Color designates group (blue: restricted, grey: control). In A), red dots identify the strain energy stored and normalized fiber length in the pre-jump posture. In B, C, and D each marker represents data from one individual.

the tendon was the next most explanatory variable and, like normalized muscle length, shows a positive relationship with energy storage (Figure 4B). In contrast, longer muscle optimal fascicle lengths reduced energy storage (pVal: 0.03, Table 4, Figure 4D) when evaluated as an induvial predictor, but was not a significant factor as a predictor in the full multi-parameter model. Opposite to our predictions, tendon stiffness did not significantly correlate with elastic strain energy when evaluated as an individual predictor (pVal>0.1 Table 4, Figure 4C), but did improve the explanatory power of a full model. The stepwise AIC comparison of full and reduced models found the sum of LG and MG maximum force capacity along the tendon, *sumFMax*, average optimal fascicle length,

avOFL, muscle length at activation onset, *avLenA0*, tendon stiffness and the interaction of tendon stiffness and muscle force capacity as the independent predictors that best correlated with stored elastic strain energy. The relative explanatory power of each predictor following similar patterns as seen in the individual analyses with muscle start length and force capacity showing the greatest predictive power. This full model had an R^2 of 0.93 and was over 280,000 times more likely to explain the variation in strain energy than any model with only one explanatory variable.

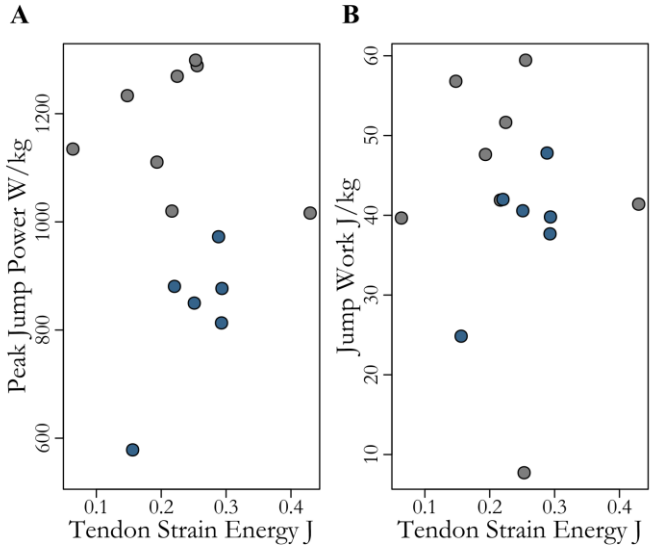

Figure 5: Neither peak jump power nor jump work increase systematically with maximum tendon strain energy across all individuals. Markers designate data from one individual in pre-jump posture and color differentiates treatment groups (grey: control, blue: restricted)

Energy storage capacity vs jump performance

We found little to no correlation between energy storage capacity predicted by simulations and experimentally collected jump metrics of either muscle mass-specific work or power (Figure 5). A linear model showed no significant relationship between either peak power jump power per kg of muscle mass capacity ($t = -036$, $p = 0.72$, Adj R^2=-0.07) or jump work ($t = -0.05$, $p = 0.96$, Adj R^2=-0.08) and strain energy in the pre-jump posture. The negative adjusted R^2 values for both tests shows that the variation in jump work or peak power explains only a negligible amount of variation in elastic energy storage potential. The scatterplot of standardized predicted values versus standardized residuals for both variables showed that the data met the assumptions of homogeneity of variance and linearity and the residuals were approximately normally distributed.

Discussion

We found the gastrocnemius elastic system of the guinea fowl robust to variations in locomotor conditions during growth. Neither properties of individual components nor energy storage capacity varied between groups of birds which did and did not jump throughout maturation. Nor did we find any correlation between energy storage capacity and jump performance. Variation in muscle operating length across individuals predicted energy storage capacity better than any fixed morphological property and a systems approach incorporating multiple components was substantially able to predict energy storage capacity better than variation along any individual element.

Do components of the gastrocnemius elastic system change systematically in response to changes in power and work demand during growth?

Contrary to our predictions, we saw, in general, no systematic changes between the gastrocnemius elastic system in response to decreased demand for high power and work activities during maturation. Surprisingly, birds that were restricted from jumping throughout their entire growth period (Table 1) developed elastic systems that were largely indistinguishable from the control group that jumped, on average, almost 200 times a day and exhibited greater peak jumping power and work at adulthood (Tables 1&2). Nor did we see differences in body mass, extensor muscle mass, tendon stiffness or leverage (moment arm and/or bone lengths).

Two factors may account for why we saw no systematic changes in the elastic system while observations of morphological plasticity in response to changes in functional demand abound [63–

67], even in guinea fowl in particular [43,68]. First, several studies suggest that plasticity may vary by life stage, with lower or inconsistent plasticity in growing animals [69–71]). Thus, the inconsistency between the lack of plasticity in our study and the morphological variation found by others suggests that guinea fowl may exhibit lower plasticity during maturation than in adulthood. Fast-growing species, like guinea fowl, might outpace environmental fluctuations with rapid growth and not invest in developmental plasticity [72,73]. A slow growing species (humans for example) might have a selective advantage with greater developmental plasticity. Thus, while our treatment may have been powerful enough to induce morphological changes in adults, rapidly growing guinea fowl may be more robust to environmental perturbations.

Second, our results could be consistent with the results of other studies if the plastic response to decreased demand is not inferable from changes in response to increases in demand. For example, it may be that the increase in muscle mass that occurs in response to a certain *increase* in functional demand is greater than the decrease in muscle mass that occurs in response to the equivalent *decrease* in demand. Many studies find clear evidence of morphological plasticity, but this was in response to increased mechanical load [24,43,66,68,74,75] and extreme disuse [76–78]. Our intervention, however, eliminated jumping and while maintaining consistent low intensity exercise (i.e. walking) and thus we did not induce chronic offloading, as had been the goal in several previous disuse studies. Our results suggest that there may not be a linear dose-response relationship between changes in functional demand and morphological variation. Instead, as recently suggested [25], there may be a range of variation in demand that is not extreme enough to induce physiological or morphological modification above those under developmental control. If this region of stasis encompasses a wider range of disuse, it could explain both why offloading studies often require extreme disuse, like bedrest or limb immobilization [76,77,79], to induce change and why we found

371 no systematic morphological changes here. Eliminating jumping may not be an extreme enough
372 disuse signal to induce musculoskeletal plasticity.
373
374 Thus, while we found no systematic morphological variation when restricting high power activities
375 during maturation, this does not necessarily imply that the morphology of elastic systems does not
376 plastically adapt to variations in functional demand. But it does suggest that there are conditions in
377 which elastic systems may be insensitive to functional variation.
378
379 **Is the energy storage capacity reduced in individuals that did not jump during growth?**
380 Despite this lack of consistent morphological variation between our treatment groups, restricted
381 birds generated lower absolute and muscle-mass-specific power and work during jumping. This
382 suggests either that small morphological changes in individual elastic elements compound to alter
383 elastic system function, that variations are significant in other MTU's that we did not quantify, or
384 that behavioral or neural variation account for the difference in jumping performance. Our systems
385 level analysis aimed to specifically address the question of whether morphological variation
386 compound within the elastic system to enable unrestricted birds to store more energy in their
387 Achilles tendon in preparation for a jump. Again, contrary to our predictions, simulations in our
388 subject-specific models resulted in no differences between groups in their ability to store elastic
389 energy. Taken together, the finding of minimal changes to individual muscle-tendon unit
390 components, and no effect on the overall elastic energy storage, could indicate that morphology
391 necessary to enable jumping is highly conserved. This could happen if rapid movements are very
392 critical to fitness, as may be the case for prey animals for whom evasion is critical.

Which type of morphological variation has the greatest influence on energy storage capacity?

The first two analyses focus on plasticity of elastic systems and quantified the influence of rearing conditions on the morphology of individual components and how that variation influenced energy storage capacity across treatment groups. Our last two analyses utilize the variation within and across our treatment groups to further probe the relationship between form and function in elastic systems.

Evaluating the best predictors of energy storage, we found that muscle properties far outweighed the influence of tendon stiffness. Surprisingly, maximum isometric muscle force, while correlating with energy storage, was not the most important factor. Instead, normalized muscle length at the start of contraction was the best individual predictor of energy storage, with the longest normalized muscle lengths enabling greatest elastic storage [(in agreement with results from [28,80]]. This may be because muscles that start contracting on the descending or plateau region of the force length curve increase force capacity as they shorten, resulting in a greater equilibrium force, while muscles starting on the ascending limb of the force-length curve lose force capacity as they shorten against a tendon during an isometric contraction [58]. Further, we were particularly surprised to find that tendon stiffness alone had little to no predictive power of energy storage. Together these data suggest that, between individuals or across an individual's lifetime, the large variation in force capacity due to force-length or force velocity effects may overshadow the influence of variation in tendon properties in determining tendon strain energy. This conclusion is consistent with studies in humans that found no correlation between tendon stiffness and vertical jump height [40]. Yet, this idea runs contrary to the focus on spring properties [23,27,39,81–85] or relative spring and maximal muscle properties [3,75] in many studies that try to connect form and function in elastic systems. Our

results suggest that instead, between or within individuals, elastic energy storage capacity may be more sensitive to variations that alter muscle operating lengths (tendon slack length, optimal fascicle lengths, joint postures) or cross-sectional area than changes in the tendons themselves.

Further, our results also highlight the importance of analyzing the components of an elastic system in concert rather than trying to infer performance from variation in one component. Our full model that included both muscle (max muscle force and starting length) and tendon properties explained changes in energy storage capacity over 280,000 times better than variation in any individual property, even when penalizing models for complexity. This, again, emphasizes the limitations of reductionist approaches to understanding how musculoskeletal morphological variation influences the energy storage capacity of an elastic system.

Does elastic energy storage capacity predict peak jump powers and work?

The finding that maximum energy storage capacity of the gastrocnemius elastic system did not predict jump performance further supports the conclusion of the need to switch our focus from individual elements to analyzing the elastic system encompassing both morphology and neural control. Contrary to our expectations, individuals who developed elastic systems capable of storing greater energy in their tendons did not take advantage of that ability to produce more powerful jumps. This suggests that morphology may play a smaller role than neural control in determining contribution of elastic energy storage in jumping. Musculoskeletal morphological variation may not be the main factor limiting jump performance.

435 The interaction between tendon and muscle force-length curves may, in part, provide a mechanistic
436 explanation for this disconnect between morphology and performance. Here we include a
437 conceptual diagram to illustrate this (Figure 6). If we plot the muscle and tendon force-length curves
438 on the same figure, it is possible to visualize how they might interact. If the muscle operates on the
439 ascending or plateau region of the force length curve where passive forces are minimal, and we
440 assume that there is no slack in the tendon, a tendon strain of zero will coincide with the muscle
441 length at the start of a contraction. Any tendon strain, then, is equal and opposite to the change in
442 muscle length. During a fixed end contraction, the maximal tendon strain occurs when the tendon
443 force equals the total muscle force of the three heads of the gastrocnemius (empty circles, Figure 6).
444 The tendon strain at equilibrium, then, is dramatically influenced by the length of the muscle when it
445 begins to contract (Figure 6A), reaching higher values for contractions starting at longer muscle
446 lengths. As our results suggest (and as can be visualized by comparing the differences in the areas of

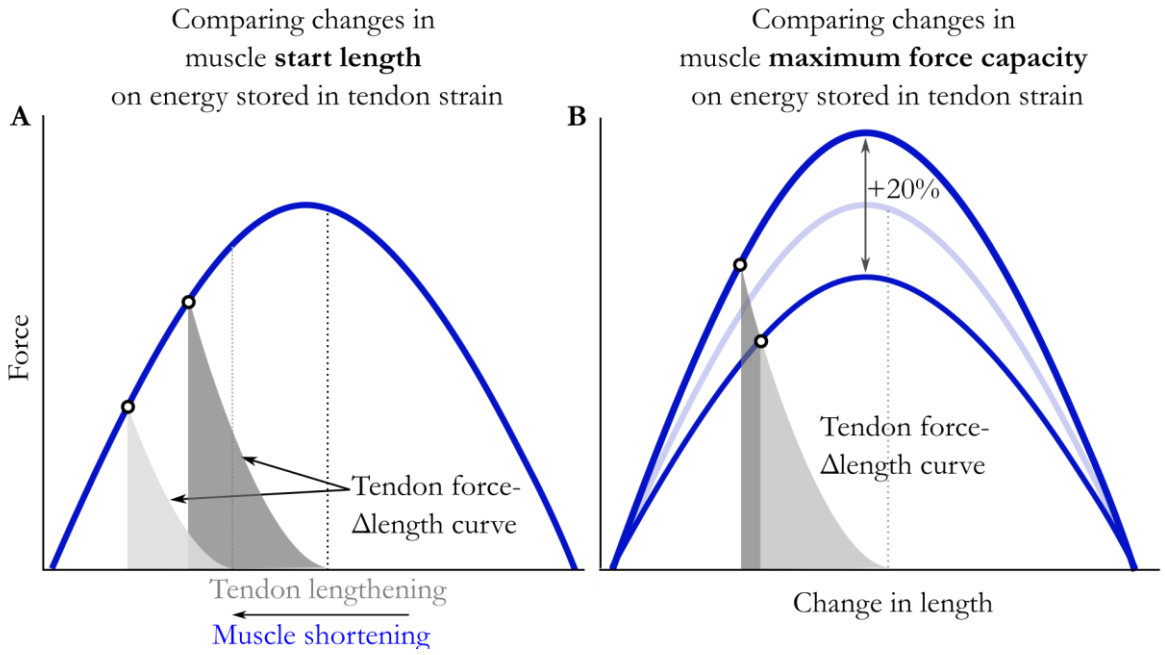

Figure 6: The energy stored in the tendon during a fixed end contraction is constrained by the interaction of the muscle (blue curve) and tendon force-Δ length curves (grey curve). Since tendon length changes must equal and opposite to muscle length changes, we can plot them at the same scale. Changes in muscle length at the onset of contraction (A) can have a larger influence on energy storage than variations in muscle force capacity (B). The variation in maximum muscle force depicted here represent variation observe in our subjects. Here changes in start length (`0.9-1.2) and muscle force capacity (±10%) reflect experimentally measured variation in our population.

the grey shaded regions between Figure 6A and B), these dynamics can be larger than the influence of naturally occurring variations in maximal force capacity (Figure 6B). And while muscle operating lengths are constrained by morphology (OFL, pennation angle and moment arms), they are also easily varied with joint angle. Large variations in maximum muscle force could be compensated for by small variations in posture largely under neural control. Thus, as our results suggest, dynamic factors like muscle operating length may influence energy storage more than temporarily fixed musculoskeletal features like maximum muscle force capacity.

This suggests that there may be a large range of morphological variation that can be compensated for with neural plasticity and brings up questions of how the two interact. Does variation along a particular morphological axis correlate with systematic changes in neural control? If so, how do individuals search though the neural possibility space? What are the limits of neural compensation? Do we see greater morphological plasticity of the components of elastic systems in conditions that push the limits of neural plasticity?

Potential interactions between musculoskeletal and neural variation in elastic energy storage

This possible sensitivity of performance to muscle operating lengths also suggests directions for further studies exploring the interaction between morphological and neural or kinematic variation. Here we assumed a uniform pre-jump posture across individuals based on measured average values [31]. Yet our results suggest variations in posture between individuals may play an important role in understanding the relationship between form and function in elastic systems. For instance, one could explore whether individuals with shorter muscle operating lengths adopt a less flexed posture to enable greater tendon energy storage in preparation for a jump. Likewise, the addition of a counter movement proceeding a jump, not common in guinea fowl [31,37] but present in many

other species [86,87], could minimize influence of muscle constraints on energy storage. This dependence of performance on the interaction between morphology and neural control again reinforces the need to expand our scope from that of the muscle-tendon unit to that of the elastic system.

Therefore, while musculoskeletal morphology may set the bounds of possible energy storage, individuals may not operate at their limits of elastic potential. This suggests either a significant behavioral component (restricted birds simply may have not tried as hard to jump) or that there may be benefits to real-time tunability in elastic systems. The jump of a guinea fowl is powered both by tendon recoil and simultaneous muscle work [31], as is common in many larger animals [86–89]. The muscles that load the tendon pre-jump also contract during takeoff to contribute power to the jump. In these hybrid systems, trade-offs between maximizing tendon strain energy and muscle power may explain our findings that the pre-jump posture of guinea fowl did not optimize energy storage in the tendon. Adjusting muscle lengths to maximize tendon strain may hamper muscles fiber work during takeoff. Further, in a complex system such as this, with dozens of individual muscle-tendon units spanning multiple joints and working in concert with direct drive muscles with little tendon, the difference between a great jumper and a good jumper might depend less on the maximal storage capacity of any one muscle tendon unit (i.e. its musculoskeletal morphology) and more on fine adjustments of neural control to harmonize the output of the collective system [90–92].

Together, our experimental and modeling analyses suggest that performance advantage of the control birds, who practiced jumping throughout maturation, may lie less in the body's modification of individual elastic elements, and instead, in the fine tuning of neural circuits to coordinate muscle activation timing to take better advantage of what they each possess. While restricting normal locomotor behavior during growth (i.e., eliminating practice) likely leads to deficits in neural control,

494 neural plasticity is potentially a rapidly reversible pathway to adapt an elastic system to functional
495 variation. Given the potential short timescale of neural plasticity [92,93], greater sensitivity of neural
496 locomotor/movement stimuli could allow the individual to adjust the dynamics of an elastic system
497 during growth without making potentially irreversible changes to morphology that could be
498 detrimental in subsequent stages of growth or in adulthood if environmental conditions or
499 functional demand rapidly change. Thus, one could interpret the results of our study as suggesting
500 that practice during growth may indeed be more related to forming the neural framework for
501 jumping than for forming the musculoskeletal framework. This also suggests the specific hypothesis
502 that individuals restricted from an activity during growth may be capable of reversing the resulting
503 neural deficits with practice later in life.

504 **Limitations**

505 Several modeling simplifications could have influenced our results. For instance, the gastrocnemius
506 elastic system is not the only one that could contribute to jump power. While the Achilles is the
507 largest tendon involved, many other digital tendons spanning both the ankle and tarsometatarsus
508 joint have the potential to contribute to jump power but were not included in our analysis
509 Furthermore, changes in the characteristics of muscles spanning proximal joints may also have
510 contributed to the differences in jump power but these muscles were not modeled. Additionally,
511 potentially important dynamic effects were ignored. For simplicity, we simulated the amount of
512 energy stored in the Achilles tendon during fixed-end contractions, where the joint posture was
513 constant as the muscle and tendon dynamically responded to increasing muscle activation.
514 Activating muscles while altering joint posture would alter these dynamics, perhaps amplifying the
515 influence of individual differences in input or output lever lengths or force-velocity effects not
516 apparent from group averages. Likewise, we did not measure and include individual variation in

517 muscle/aponeurosis passive elastic properties that could significantly alter energy storage [36,94,95].
518 While this is a common approach in musculoskeletal modeling [50,60,96], variation in the
519 aponeurosis and free tendon stiffness [97,98] have the potential to introduce errors [16,99].

520 Another possible limitation was the modeling choice to focus on the potential for an individual to
521 store energy in the strain of their tendon. How that energy is released and how that energy release
522 interacts with synchronous muscle activation could also influence jump performance [5]. Because
523 jumps are likely powered both by tendon recoil and muscle work [31,80], there may be a tradeoff
524 between the work the muscle puts into tendon strain and that which is left available to power the
525 jump during tendon recoil [100]. Future work could involve simulation of jumps in these subject-
526 specific models to assess the contributions of these dynamic factors. Thus, while we found no
527 consistent change in components of the gastrocnemius elastic system due to decreased demand for
528 high power activities during growth, more complex models may provide insight into the ways in
529 which morphological variation constrains performance.

530 **Summary**

531 We found that decreasing the demand for high power and work during growth can influence adult
532 performance but does not necessarily lead to morphological plasticity. We found no difference in
533 energy storage capacity between groups which did and did not jump throughout maturation or any
534 correlation with experimentally measured jump performance. We conclude that gastrocnemius
535 elastic system in the guinea fowl displays little to no morphological plastic response to decreased
536 demand during growth and that neural control of elastic systems may constrain performance more
537 than morphology.

538 ## Author Contributions

SMC, JR, SJP, MQS contributed to the conception and design of the study. JR, MQS, SJP and SMC developed methodologies and KK, AD, MQS, SMC collected the data. SMC, MQS analyzed the data and SMC prepared the figures. SMC and JR drafted the initial manuscript. All authors contributed to manuscript editing and approved the final manuscript.

Funding

This study was supported in part through a seed grant from the Center for Human Evolution and Diversity, The Pennsylvania State University, and through the National Institute of Arthritis and Musculoskeletal and Skin Diseases of the National Institutes of Health under grant number R21AR071588. The content is solely the responsibility of the authors of this paper and does not necessarily represent the views of the National Institutes of Health.

Conflict of Interest

The authors declare that the research was conducted in the absence of any commercial or financial relationships that could be construed as a potential conflict of interest.

Data Availability

TBD

References

1. Patek SN, Dudek DM, Rosario M V. 2011 From bouncy legs to poisoned arrows: Elastic movements in invertebrates. *J. Exp. Biol.* **214**, 1973–1980. (doi:10.1242/jeb.038596)

2. Roberts TJ, Azizi E. 2011 Flexible mechanisms: the diverse roles of biological springs in vertebrate movement. *J. Exp. Biol.* **214**, 353–61. (doi:10.1242/jeb.038588)

559 3. Lichtwark GA, Wilson AM. 2008 Optimal muscle fascicle length and tendon stiffness for
560 maximising gastrocnemius efficiency during human walking and running. *J. Theor. Biol.* **252**,
561 662–673. (doi:10.1016/j.jtbi.2008.01.018)

562 4. Wilson AM, Van den Bogert AJ, McGuigan MP. 2000 Optimization of the muscle-tendon
563 unit for economical locomotion. In *Skeletal muscle mechanics: from mechanism to function* (ed W
564 Herzog), pp. 517–47. Hoboken, NJ: John Wiley & Sons.

565 5. Ilton M *et al.* 2018 The principles of cascading power limits in small, fast biological and
566 engineered systems. *Science (80-.).* **360**. (doi:10.1126/science.aao1082)

567 6. Richards CT, Sawicki GS. 2012 Elastic recoil can either amplify or attenuate muscle-tendon
568 power, depending on inertial vs. fluid dynamic loading. *J. Theor. Biol.* **313**, 68–78.
569 (doi:10.1016/j.jtbi.2012.07.033)

570 7. Astley HC, Roberts TJ. 2014 The mechanics of elastic loading and recoil in anuran jumping.
571 *J. Exp. Biol.* **217**, 4372–4378. (doi:10.1242/jeb.110296)

572 8. Astley HC, Roberts TJ. 2012 Evidence for a vertebrate catapult: elastic energy storage in the
573 plantaris tendon during frog jumping. *Biol. Lett.* **8**, 386–9. (doi:10.1098/rsbl.2011.0982)

574 9. Galantis A, Woledge RC. 2003 The theoretical limits to the power output of a muscle –
575 tendon complex with inertial and gravitational loads. , 1493–1498.
576 (doi:10.1098/rspb.2003.2403)

577 10. Robertson BD, Sawicki GS. 2014 Exploiting elasticity: Modeling the influence of neural
578 control on mechanics and energetics of ankle muscle-tendons during human hopping. *J.*
579 *Theor. Biol.* **353**, 121–132. (doi:10.1016/j.jtbi.2014.03.010)

580 11. Sawicki GS, Robertson BD, Azizi E, Roberts TJ. 2015 Timing matters: tuning the mechanics
581 of a muscle-tendon unit by adjusting stimulation phase during cyclic contractions. *J. Exp. Biol.*
582 **218**, 3150–3159. (doi:10.1242/jeb.121673)

583 12. Nishikawa K *et al.* 2007 Neuromechanics : an integrative approach for understanding motor
584 control. **47**, 16–54. (doi:10.1093/icb/icm024)

585 13. Gillis GB, Biewener AA. 2001 Hindlimb muscle function in relation to speed and gait: in vivo
586 patterns of strain and activation in a hip and knee extensor of the rat (Rattus norvegicus). *J.*
587 *Exp. Biol.* **204**, 2717–2731.

588 14. Lutz GJ, Rome LC. 1996 Muscle function during jumping in frogs. I. Sarcomere length
589 change, EMG pattern, and jumping performance. *Am. J. Physiol.* **271**, C563-70.

590 15. Kao P-C, Lewis CL, Ferris DP. 2010 Short-term locomotor adaptation to a robotic ankle
591 exoskeleton does not alter soleus Hoffmann reflex amplitude. *J. Neuroeng. Rehabil.* **7**, 33.
592 (doi:10.1186/1743-0003-7-33)

593 16. Lieber RL, Roberts TJ, Blemker SS, Lee SSM, Herzog W. 2017 Skeletal muscle mechanics,
594 energetics and plasticity. *J. Neuroeng. Rehabil.* **14**, 108. (doi:10.1186/s12984-017-0318-y)

595 17. Du TY, Standen EM. 2017 Phenotypic plasticity of muscle fiber type in the pectoral fins of
596 Polypterus senegalus reared in a terrestrial environment . *J. Exp. Biol.* **220**, 3406–3410.
597 (doi:10.1242/jeb.162909)

598 18. Estes RR, Malinowski A, Piacentini M, Thrush D, Salley E, Losey C, Hayes E. 2017 The
599 Effect of High Intensity Interval Run Training on Cross-sectional Area of the Vastus
600 Lateralis in Untrained College Students. *Int. J. Exerc. Sci.* **10**, 137–145.

19. Iadecola C, Anrather J, Medical WC. 2015 Dramatic changes in muscle contractile and structural properties after two Botulinum toxin injections. *Muscle and Nerve* **52**, 649–657. (doi:10.1038/nm.2399.The)

20. Bohm S, Mersmann F, Tettke M, Kraft M, Arampatzis A. 2014 Human Achilles tendon plasticity in response to cyclic strain : effect of rate and duration. , 4010–4017. (doi:10.1242/jeb.112268)

21. Docking SI, Cook J. 2019 How do tendons adapt? Going beyond tissue responses to understand positive adaptation and pathology development: A narrative review. *J. Musculoskelet. Neuronal Interact.* **19**, 300–310.

22. Eliasson P, Fahlgren A, Pasternak B, Aspenberg P. 2007 Unloaded rat Achilles tendons continue to grow, but lose viscoelasticity. *J. Appl. Physiol.* **103**, 459–463. (doi:10.1152/japplphysiol.01333.2006)

23. Bohm S, Mersmann F, Arampatzis A. 2019 Functional adaptation of connective tissue by training. *Dtsch. Z. Sportmed.* **70**, 105–109. (doi:10.5960/dzsm.2019.366)

24. Kubo K, Morimoto M, Komuro T, Yata H, Tsunoda N, Kanehisa H, Fukunaga T. 2007 Effects of Plyometric and Weight Training on Muscle–Tendon Complex and Jump Performance. *Med. Sci. Sport. Exerc.* **39**, 1801–1810. (doi:10.1249/mss.0b013e31813e630a)

25. Katugam K, Cox SM, Salzano MQ, De Boef A, Hast MW, Neuberger T, Ryan TM, Piazza SJ, Rubenson J. 2020 Altering the Mechanical Load Environment During Growth Does Not Affect Adult Achilles Tendon Properties in an Avian Bipedal Model. *Front. Bioeng. Biotechnol.* **8**. (doi:10.3389/fbioe.2020.00994)

26. Mayfield DL, Launikonis BS, Cresswell AG, Lichtwark GA. 2016 Additional in-series

623 compliance reduces muscle force summation and alters the time course of force relaxation
624 during fixed-end contractions. *J. Exp. Biol.* **219**, jeb.143123. (doi:10.1242/jeb.143123)

625 27. Albracht K, Arampatzis A. 2006 Influence of the mechanical properties of the muscle-tendon
626 unit on force generation in runners with different running economy. *Biol. Cybern.* **95**, 87–96.
627 (doi:10.1007/s00422-006-0070-z)

628 28. Rosario M V, Sutton GP, Patek SN, Sawicki GS. 2016 Muscle – spring dynamics in time-
629 limited, elastic movements. *Proc. R. Soc. B* **283**, 20161561.
630 (doi:10.6084/m9.figshare.c.3462654.)

631 29. Zajac FE. 1992 How musculotendon architecture and joint geometry affect the capacity of
632 muscles to move and exert force on objects: A review with application to arm and forearm
633 tendon transfer design. *J. Hand Surg. Am.* **17**, 799–804. (doi:10.1016/0363-5023(92)90445-U)

634 30. Ettema GJC. 1996 Elastic and length-force characteristics of the gastrocnemius of the
635 hopping mouse (Notomys alexis) and the rat (Rattus norvegicus). *J. Exp. Biol.* **199**, 1277–
636 1285.

637 31. Henry HT, Ellerby DJ, Marsh RL. 2005 Performance of guinea fowl Numida meleagris
638 during jumping requires storage and release of elastic energy. *J. Exp. Biol.* **208**, 3293–3302.
639 (doi:10.1242/jeb.01764)

640 32. Alexander R. 1968 *Animal Mechanics*. University of Washington Press.

641 33. Biewener AA, Mcgowan C, Card GM, Baudinette R V. 2004 Dynamics of leg muscle
642 function in tammar wallabies (M . eugenii) during level versus incline hopping. , 211–223.
643 (doi:10.1242/jeb.00764)

644 34. Walmsley B, Hodgson JA, Burke RE. 1978 Forces produced by medial gastrocnemius and
645 soleus muscles during locomotion in freely moving cats. *J. Neurophysiol.* **41**, 1203–1216.
646 (doi:10.1152/jn.1978.41.5.1203)

647 35. Farris DJ, Lichtwark GA, Brown NAT, Cresswell AG. 2016 The role of human ankle plantar
648 flexor muscle-tendon interaction and architecture in maximal vertical jumping examined in
649 vivo. *J. Exp. Biol.* **219**, 528–534. (doi:10.1242/jeb.126854)

650 36. Arellano CJ, Konow N, Gidmark NJ, Roberts TJ. 2019 Evidence of a tunable biological
651 spring: Elastic energy storage in aponeuroses varies with transverse strain in vivo. *Proc. R. Soc.*
652 *B Biol. Sci.* **286**, 3–8. (doi:10.1098/rspb.2018.2764)

653 37. Cox SM, Salzano MQ, Piazza SJ, Rubenson J. 2020 Eliminating high-intensity activity during
654 growth reduces mechanical power capacity but not submaximal metabolic cost in a bipedal
655 animal model. *J. Appl. Physiol.* **128**, 50–58. (doi:10.1152/japplphysiol.00679.2019)

656 38. Biewener A a, Baudinette R. 1995 In vivo muscle force and elastic energy storage during
657 steady-speed hopping of tammar wallabies (Macropus eugenii). *J. Exp. Biol.* **198**, 1829–41.

658 39. Biewener AA, Roberts TJ. 2000 Muscle and tendon contributions to force, work, and elastic
659 energy savings: a comparative perspective. *Excersice Sport Sci. Rev.* **28**, 99–107. (doi:10916700)

660 40. Kubo K, Kawakami Y, Fukunaga T, Kawakami Y, Fuku- T. 2019 Influence of elastic
661 properties of tendon structures on jump performance in humans. , 2090–2096.

662 41. Rubenson J, Marsh RL. 2009 Mechanical efficiency of limb swing during walking and running
663 in guinea fowl (Numida meleagris). *J. Appl. Physiol.* **106**, 1618–1630.
664 (doi:10.1152/japplphysiol.91115.2008)

42. Rubenson J, Henry HT, Dimoulas PM, Marsh RL. 2006 The cost of running uphill : linking organismal and muscle energy use in guinea fowl (Numida meleagris). *J. Exp. Biol.* **209**, 2395–2408. (doi:10.1242/jeb.02310)

43. Salzano MQ, Cox SM, Piazza SJ, Rubenson J. 2018 American Society of Biomechanics Journal of Biomechanics Award 2017: High-acceleration training during growth increases optimal muscle fascicle lengths in an avian bipedal model. *J. Biomech.* **80**, 1–7. (doi:10.1016/j.jbiomech.2018.09.001)

44. Azizi E, Deslauriers AR. 2014 Regional heterogeneity in muscle fiber strain: the role of fiber architecture. *Front. Physiol.* **5**, 303. (doi:10.3389/fphys.2014.00303)

45. Ahn AN, Monti RJ, Biewener AA. 2003 In vivo and in vitro heterogeneity of segment length changes in the semimembranosus muscle of the toad. *J. Physiol.* **549**, 877–888. (doi:10.1113/jphysiol.2002.038018)

46. Carr JA, Ellerby DJ, Marsh RL. 2011 Differential segmental strain during active lengthening in a large biarticular thigh muscle during running. *J. Exp. Biol.* **214**, 3386–95. (doi:10.1242/jeb.050252)

47. Buchanan TS, Lloyd DG, Manal K, Besier TF. 2004 Neuromusculoskeletal modeling: Estimation of muscle forces and joint moments and movements from measurements of neural command. *J. Appl. Biomech.* **20**, 367–395. (doi:10.1016/j.bbi.2008.05.010)

48. Mendez J, Keys A. 1960 Density and Composition of Mammalian Muscle. Metabolism, 9, 184-188. - References - Scientific Research Publishing. See https://www.scirp.org/(S(lz5mqp453edsnp55rrgjct55))/reference/ReferencesPapers.aspx?ReferenceID=1219605 (accessed on 19 August 2020).

687 49. Rospars JP, Meyer-Vernet N. 2016 Force per cross-sectional area from molecules to muscles:
688 A general property of biological motors. *R. Soc. Open Sci.* **3**. (doi:10.1098/rsos.160313)

689 50. Millard M, Uchida T, Seth A, Delp SL. 2013 Flexing Computational Muscle: Modeling and
690 Simulation of Musculotendon Dynamics. *J. Biomech. Eng.* **135**, 021005.
691 (doi:10.1115/1.4023390)

692 51. Spoor CW, van Leeuwen JL. 1992 Knee muscle moment arms from MRI and from tendon
693 travel. *J. Biomech.* **25**, 201–206. (doi:10.1016/0021-9290(92)90276-7)

694 52. Landsmeer JM. 1961 Studies in the anatomy of articulation. 1. The equilibrium of the
695 'intercalated' bone. *Acta Morphol. Neerl. Scand.* **3**, 287–303.

696 53. Salzano M. 2020 Musculoskeletal Plasticity in Response to Loading History during Growth.
697 The Pennsylvania State University.

698 54. Lewis GS, Sommer HJ, Piazza SJ. 2006 In vitro assessment of a motion-based optimization
699 method for locating the talocrural and subtalar joint axes. *J. Biomech. Eng.* **128**, 596–603.
700 (doi:10.1115/1.2205866)

701 55. De Groote F, Van Campen A, Jonkers I, De Schutter J. 2010 Sensitivity of dynamic
702 simulations of gait and dynamometer experiments to hill muscle model parameters of knee
703 flexors and extensors. *J. Biomech.* **43**, 1876–1883. (doi:10.1016/j.jbiomech.2010.03.022)

704 56. Ackland DC, Lin YC, Pandy MG. 2012 Sensitivity of model predictions of muscle function
705 to changes in moment arms and muscle-tendon properties: A Monte-Carlo analysis. *J.*
706 *Biomech.* **45**, 1463–1471. (doi:10.1016/j.jbiomech.2012.02.023)

707 57. Scovil CY, Ronsky JL. 2006 Sensitivity of a Hill-based muscle model to perturbations in

model parameters. *J. Biomech.* **39**, 2055–2063. (doi:10.1016/j.jbiomech.2005.06.005)

58. Cox SM *et al.* 2019 The Interaction of Compliance and Activation on the Force-Length Operating Range and Force Generating Capacity of Skeletal Muscle: A Computational Study using a Guinea Fowl Musculoskeletal Model. *Integr. Org. Biol.* **1**, 1–20. (doi:10.1093/iob/obz022)

59. Venables WN, Ripley BD. 2002 *Modern Applied Statistics with S*. 4th edn. New York: Springer-Verlag.

60. Zajac FE. 1989 Muscle and tendon: properties, models, scaling, and application to biomechanics and motor control. *Crit. Rev. Biomed. Eng.* **17**, 359–411. (doi:10.1016/j.pcad.2015.11.006)

61. Wagenmakers E-J, Farrell S. 2004 AIC model selection using Akaike weights. *Psychon. Bull. Rev.* **11**, 192–6.

62. Cox S, Salzano M, DeBoef A, Piazza S, Rubenson J. 2019 Decreased physical activity during growth reduces peak force capacity but not running economy in a bipedal animal model. In *International Society of Biomechanics*, Calgary, Canada.

63. Blazevich AJ, Gill ND, Bronks R, Newton RU. 2003 Training-Specific Muscle Architecture Adaptation after 5-wk Training in Athletes. *Med. Sci. Sports Exerc.* **35**, 2013–2022. (doi:10.1249/01.MSS.0000099092.83611.20)

64. Baldwin KM, Haddad F. 2002 Skeletal muscle plasticity: Cellular and molecular responses to altered physical activity paradigms. *Am. J. Phys. Med. Rehabil.* **81**, 40–51. (doi:10.1097/00002060-200211001-00006)

729 65. Fitts RH, Widrick JJ. 1996 Muscle Mechanics: Adapations with exercise-training. *Exerc. Sport*
730 *Sci. Rev.* **24**, 427–474.

731 66. Mcdonagh MJN, Davies CTM. 1984 Adaptive response of mammalian skeletal muscle to
732 exercise with high loads. *Eur. J. Appl. Physiol.* **52**, 139–155.

733 67. Wisdom KM, Delp SL, Kuhl E. 2015 Use it or lose it: multiscale skeletal muscle adaptation to
734 mechanical stimuli. *Biomech. Model. Mechanobiol.* **14**, 195–215. (doi:10.1007/s10237-014-0607-3)

735 68. Buchanan CI, Marsh RL. 2001 Effects of long-term exercise on the biomechanical properties
736 of the Achilles tendon of guinea fowl. *J Appl Physiol* **90**, 164–171.

737 69. Legerlotz K, Marzilger R, Bohm S, Arampatzis A. 2016 Physiological Adaptations following
738 Resistance Training in Youth Athletes—A Narrative Review. *Pediatr. Exerc. Sci.* **28**, 501–520.
739 (doi:10.1123/pes.2016-0023)

740 70. Johnston IA. 2006 Environment and plasticity of myogenesis in teleost fish. *J. Exp. Biol.* **209**,
741 2249–2264. (doi:10.1242/jeb.02153)

742 71. Aucouturier J, Baker JS, Duché P. 2008 Fat and carbohydrate metabolism during submaximal
743 exercise in children. *Sport. Med.* **38**, 213–238. (doi:10.2165/00007256-200838030-00003)

744 72. Dewitt TJ, Sih a, Wilson DS. 1998 Costs and limits of phenotypic plasticity. *Trends Ecol. Evol.*
745 **13**, 77–81.

746 73. Snell-Rood EC. 2012 Selective processes in development: Implications for the costs and
747 benefits of phenotypic plasticity. *Integr. Comp. Biol.* **52**, 31–42. (doi:10.1093/icb/ics067)

748 74. Atherton PJ, Smith K. 2012 Muscle protein synthesis in response to nutrition and exercise. *J.*
749 *Physiol.* **590**, 1049–1057. (doi:10.1113/jphysiol.2011.225003)

750 75. Mersmann F, Charcharis G, Bohm S, Arampatzis A. 2017 Muscle and tendon adaptation in
751 adolescence: Elite volleyball athletes compared to untrained boys and girls. *Front. Physiol.* **8**.
752 (doi:10.3389/fphys.2017.00417)

753 76. Bajotto G, Shimomura Y. 2007 Determinants of Disuse-Induced Skeletal Muscle Atrophy:
754 Exercise and Nutrition Countermeasures to Prevent Protein Loss. *J. Nutr. Sci. Vitaminol.*
755 *(Tokyo).* **52**, 233–247. (doi:10.3177/jnsv.52.233)

756 77. Clark BC. 2009 In vivo alterations in skeletal muscle form and function after disuse atrophy.
757 *Med. Sci. Sports Exerc.* **41**, 1869–1875. (doi:10.1249/MSS.0b013e3181a645a6)

758 78. Campbell EL, Seynnes OR, Bottinelli R, McPhee JS, Atherton PJ, Jones DA, Butler-Browne
759 G, Narici M V. 2013 Skeletal muscle adaptations to physical inactivity and subsequent
760 retraining in young men. *Biogerontology* **14**, 247–259. (doi:10.1007/s10522-013-9427-6)

761 79. Bebout DE, Hogan MC, Hempleman SC, Wagner PD. 1993 Effects of training and
762 immobilization on VO2 and DO2 in dog gastrocnemius muscle in situ. *J. Appl. Physiol.* **74**,
763 1697–703.

764 80. Azizi E, Roberts TJTTJ. 2010 Muscle performance during frog jumping: influence of
765 elasticity on muscle operating lengths. *Proc. A R. Soc. B* **277**, 1523–1530.
766 (doi:10.1098/rspb.2009.2051)

767 81. Waugh CM, Blazevich AJ, Fath F, Korff T. 2012 Age-related changes in mechanical
768 properties of the Achilles tendon. *J. Anat.* **220**, 144–155. (doi:10.1111/j.1469-
769 7580.2011.01461.x)

770 82. Khayyeri H, Blomgran P, Hammerman M, Turunen MJ, Löwgren A, Guizar-Sicairos M,
771 Aspenberg P, Isaksson H. 2017 Achilles tendon compositional and structural properties are

altered after unloading by botox. *Sci. Rep.* **7**, 1–10. (doi:10.1038/s41598-017-13107-7)

83. Fletcher JR, MacIntosh BR. 2018 Changes in Achilles tendon stiffness and energy cost following a prolonged run in trained distance runners. *PLoS One* **13**, 1–17. (doi:10.1371/journal.pone.0202026)

84. Proske U, Morgan DL. 1987 Tendon stiffness: Methods of measurement and significance for the control of movement. A review. *J. Biomech.* **20**, 75–82. (doi:10.1016/0021-9290(87)90269-7)

85. Waugh CM, Korff T, Fath F, Blazevich AJ. 2014 Effects of resistance training on tendon mechanical properties and rapid force production in prepubertal children. *J. Appl. Physiol.* **117**, 257–266. (doi:10.1152/japplphysiol.00325.2014)

86. Kubo K, Kawakami Y, Fukunaga T. 1999 Influence of elastic properties of tendon structures on jump performance in humans. *J. Appl. Physiol.* **87**, 2090–2096. (doi:10.1152/jappl.1999.87.6.2090)

87. Alexander RM. 1995 Leg design and jumping technique for humans, other vertebrates and insects. *Philos. Trans. R. Soc. Lond. B. Biol. Sci.* **347**, 235–248. (doi:10.1098/rstb.1995.0024)

88. Alexander RM. 1974 The mechancs of jumping by a dog. *J. Zool.* **173**, 549–573.

89. Roberts TJ. 2003 Probing the limits to muscle-powered accelerations: lessons from jumping bullfrogs. *J. Exp. Biol.* **206**, 2567–2580. (doi:10.1242/jeb.00452)

90. Häkkinen K, Alen M, Kallinen M, Newton R, Kraemer W. 2000 Neuromuscular adaptation during prolonged strength training, detraining and re-strength-training in middle-aged and elderly people. *Eur. J. Appl. Physiol.* **83**, 51–62. (doi:10.1007/s004210000248)

91. Enoka RM. 1997 Neural Adapations with Chronic physical activity. *J. Biomech.* **30**, 465–475.

92. Adkins DL, Boychuk J, Remple MS, Kleim JA. 2006 Motor training induces experience-specific patterns of plasticity across motor cortex and spinal cord. *J. Appl. Physiol.* **101**, 1776–1782. (doi:10.1152/japplphysiol.00515.2006)

93. Yoxon E, Welsh TN. 2019 Rapid motor cortical plasticity can be induced by motor imagery training. *Neuropsychologia* **134**, 107206. (doi:10.1016/j.neuropsychologia.2019.107206)

94. Huijing PA, Ettema GJ. 1988 Length-force characteristics of aponeurosis in passive muscle and during isometric and slow dynamic contractions of rat gastrocnemius muscle. *Acta Morphol. Neerl. Scand.* **26**, 51–62.

95. Lemos RR, Epstein M, Herzog W. 2008 Modeling of skeletal muscle: The influence of tendon and aponeuroses compliance on the force-length relationship. *Med. Biol. Eng. Comput.* **46**, 23–32. (doi:10.1007/s11517-007-0259-x)

96. Seth A *et al.* 2018 OpenSim : Simulating musculoskeletal dynamics and neuromuscular control to study human and animal movement. *Comput. Biol.* **14**, e1006223.

97. Finni T. 2006 Structural and functional features of human muscle-tendon unit. *Scand. J. Med. Sci. Sport.* **16**, 147–158. (doi:10.1111/j.1600-0838.2005.00494.x)

98. Ettema GJC, Huijing PA. 1989 Properties of the tendinous structures and series elastic component of EDL muscle-tendon complex of the rat. *J. Biomech.* **22**, 1209–1215. (doi:10.1016/0021-9290(89)90223-6)

99. Epstein M, Wong M, Herzog W. 2006 Should tendon and aponeurosis be considered in series? *J. Biomech.* **39**, 2020–2025. (doi:10.1016/j.jbiomech.2005.06.011)

814 100. Sutton GP, Mendoza E, Azizi E, Longo SJ, Olberding JP, Ilton M, Patek SN. 2019
815 Integrative and Comparative Biology Why do Large Animals Never Actuate Their Jumps
816 with Latch- Mediated Springs ? Because They can Jump Higher Without Them. , 1–10.
817 (doi:10.1093/icb/icz145)

818 101. Winter D. 2009 *Biomechanics and motor control of human movement*. 4th edn. Hoboken, NH: John
819 Wiley & Sons, Inc.

820 102. Gollapudi SK, Lin DC. 2009 Experimental determination of sarcomere force-length
821 relationship in type-I human skeletal muscle fibers. *J. Biomech.* **42**, 2011–2016.
822 (doi:10.1016/j.jbiomech.2009.06.013)

823

824 # Appendix A

825 **Estimation of tendon slack length from experimental measures**

826 Tendon slack length was estimated from experimental measures of muscle and tendon morphology
827 as follows. First, the maximum isometric force along the tendon was calculated from the maximum
828 force along the fiber and the pennation angle at optimal fascicle length, θ_{OFL}, according to the
829 equation:

$$F_{maxT} = F_{max} \cos\theta_{OFL}. \quad (5)$$

830 The passive force of the muscle exerted on the tendon in the experimentally measured posture was
831 found from the normalized passive muscle force as a function of normalized fiber length curve,

832 $f_{np}(nFl)$ [101,102]. This was first scaled, for each muscle, by the maximum isometric force along
833 the tendon, F_{maxT},

$$f_{muscP} = F_{maxT} f_{np}(nFl). \quad (6)$$

834 By normalizing the experimentally measured average fiber length by the muscle's optimal fascicle
835 length, we could calculate the normalized fiber length of the muscle in the fixed posture, *nFl*,
836 allowing us to solve equation (4) for the passive force, f_{muscP}, each muscle exerted on the tendon in
837 the experimental posture. Since the three heads of the gastrocnemius attach to the Achilles tendon,
838 the passive force of each muscle was calculated separately and summed. As the gastrocnemius
839 intermedia head makes up ~10% of the total gastrocnemius muscle by volume, the passive
840 contribution of this muscle was not experimentally determined for each bird but was estimated from
841 values previously collected [58]. The passive force exerted by the muscle must be balanced by an
842 equal tendon force, thus, the summed passive muscle forces equal the passive force the tendon
843 experienced in the experimental posture.

844 The MTU lengths, L_{MTU}, were measured on the fixed limbs by digitizing the three-dimensional
845 paths of the MG and LG from their origins on the tibiotarsus and femur, respectively, to the
846 insertion of the Achilles tendon on the hypotarsus. This approach inherently includes the
847 aponeurosis in the overall tendon length. Digitizing was done using a digitizing arm (Microscribe
848 3DX, Immersion, San Jose, CA). The MTU path was described by 11 points. The linear distances
849 along the MTU path were summed to obtain an overall MTU length. This experimentally measured
850 MTU length, L_{MTU}, is the sum of the measured fiber length, L_M, the tendon's slack length, L_T, and
851 length change in the tendon (tendon stretch) due to passive muscle fiber force. The length change

852 in the tendon due to passive muscle fiber force can be described as the tendon strain, ε_T, times its
853 tendon slack length, L_{T0}.

$$L_{MTU} = L_M + L_T + L_T\varepsilon_T \quad (7)$$

854 The strain in the tendon due to the passive muscle fiber force, ε_T, was calculated using the
855 experimentally measured tendon force-displacement curve. The tendon force-displacement curve
856 was normalized by tendon length to generate a force-strain curve.

$$f_T = g(\varepsilon_T). \quad (8)$$

857 The strain at which the tendon force is equal to the passive fiber force can then be found from the
858 inverse of equation (6) and the passive muscle force, f_{MP} .

$$\varepsilon_T = g^{-1}(f_{MP}). \quad (9)$$

859 The tendon slack length, for each muscle, then, can be calculated from equations (5) and (7).

$$L_{T0} = \frac{L_{MTU} - L_M}{(1 + \varepsilon_T)} \quad (10)$$

860

861 # Appendix B

862 ## Development of subject specific models

863 To perform system level analyses, we modified the generic OpenSim guinea fowl model [58] to
864 generate subject-specific models for each individual. First, the generic model was scaled to match
865 the measured bone lengths and body mass for each bird and saved as distinct models. In each

subject specific model, the generic LG and MG maximum isometric force, pennation angle, optimal fascicle length and tendon slack length were modified to match the experimentally measured and calculated properties.

The moment arms of the LG and MG acting at the ankle was fit to experimental values by adjusting the of the size and orientation of the cylindrical wrapping surface for the Achilles at the ankle. During the trial-and-error fitting process, the radius, translation, and rotation of the wrap surface was modified, and the resulting moment arm was compared to the experimentally collected data at 31-34 points across the experimental range with a mean moment arm normalized root mean square of the error (Figure S1A) of 0.009±0.007.

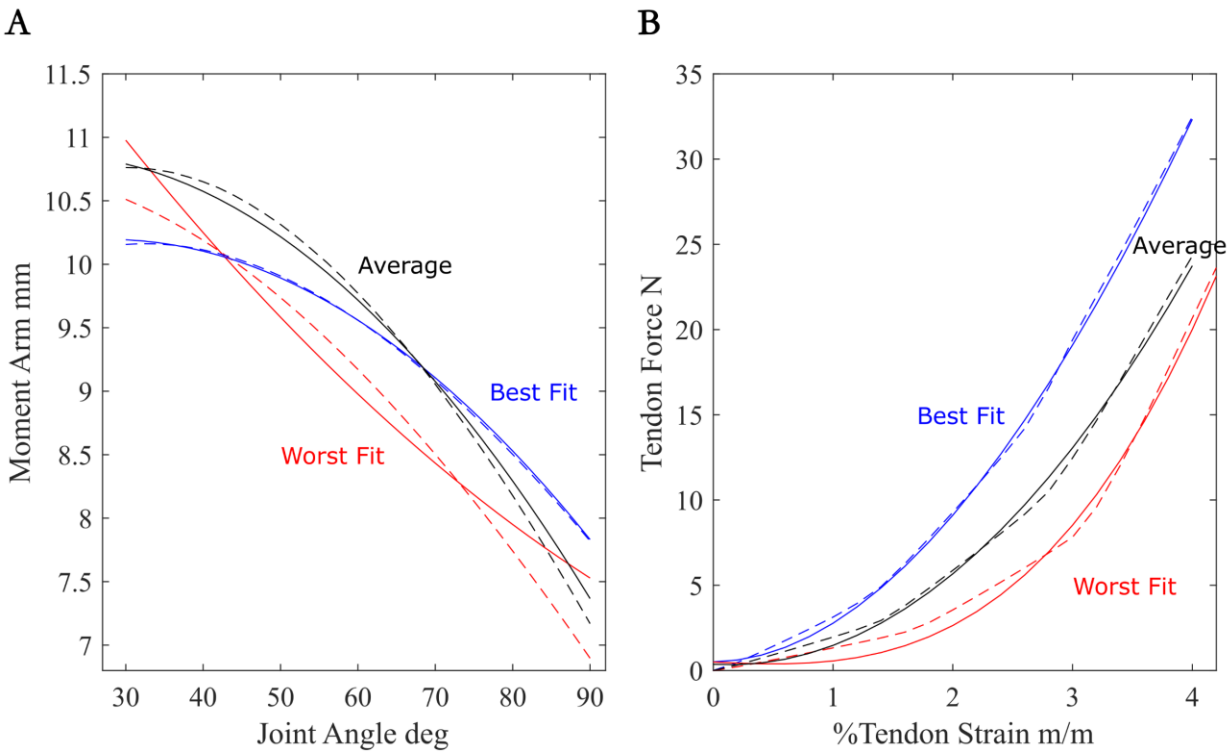

Figure S1: Example comparisons between experimental (solid lines) and modeled (dashed lines) moment arms (A) and tendon force-strain curves (B). In each plot, experimental and modeled curves are displayed for three animals, showing the best, the average and the worst fit across individuals.

875 Additionally, the tendon force-strain curve was updated to match experimentally collected force-
876 strain values. Because OpenSim scales the tendon force-strain curve by the maximum isometric
877 force of the muscle, each tendon force-strain curve was normalized by the maximum isometric force
878 capacity of the LG or MG, respectively. The parameters of the Millard muscle model's tendon force-
879 strain curve were iteratively varied for both the LG and MG and compared to the experimental
880 curve for each individual, resulting in an average root mean square error (normalized by tendon
881 force) over 26-31 points for each tendon force-length curve (Figure S1B) of 0.061+0.025.